Supplementary Information (SI) for Materials Horizons.
This journal is © The Royal Society of Chemistry 2025

Supporting information

Supersensitive natural rubber-based piezoresistive pressure sensor with hierarchical sandwich structure

Han Lu, [a] Hongfu Xie, [a] Guhuan Chen, [a] Junyi Zhang, [a] Binyu Zhu, [a] Bozhi Zhou, [a] Xuejun Lai, [a] Hongqiang Li, *[a] Xingrong Zeng [a]

School of Materials Science and Engineering, Key Lab of Guangdong Province for High Property and Functional Polymer Materials, South China University of Technology, Guangzhou 510640, China

***Corresponding authors**

Email：lihq@scut.edu.cn (H. Li)

Preparation of D-MGN sensor

300 mg of MWCNTs were ground and mixed with 80 mg of X-100 and 75 mL of deionized water, stirred at 2000 rpm for 1 h, then 5 mL of GEL solution (16 mg mL^{-1}) was slowly added and stirred for another 0.5 h. The resulting NRL/MWCNTs/GEL mixture (30 mL) was filtered under vacuum through a cellulose ester membrane to form a thin film. After washing with deionized water and soaking in acetone to dissolve the cellulose ester membrane, the film was dried at 60 °C for 1 h. The resulting NRL/MWCNTs/GEL film was cut into 10 mm×15 mm rectangles, stacked face-to-face，and the D-MGN was obtained. Two copper foils were attached on the top and bottom sides of the D-MGN as electrodes with a minimal amount of conductive silver adhesive, and the D-MGN sensor was obtained.

Preparation of P-MN_3 sensor

After grinding 300 mg of MWCNTs and cutting NR into small pieces, 2 g of NR, 1 g of MWCNTs, and 6 g of granulated NaCl particles were added to a beaker containing 30 mL of cyclohexane. The mixture was stirred at 500 rpm for 10 h to obtain an NR/MWCNTs/NaCl slurry. The slurry was uniformly applied onto a smooth glass surface (1.4 mm±0.2 mm) using a glass rod, then dried at 60 °C for 1.5 h to evaporate the cyclohexane. Subsequently, it was cut into 10 mm×15 mm rectangular film and immersed into a large amount of deionized water at 60 °C for 80 h to wash off the granulated NaCl. Two copper foils were attached on the top and bottom sides of $NR/NaCl_{1:3}$ porous film

as electrodes with a minimal amount of conductive silver adhesive, and *P-MN_3* sensor was prepared.

Preparation of P-MN_3@D-MN sensor

300 mg of MWCNTs were ground and mixed with 80 mg of X-100 and 80 mL of deionized water, stirred at 2000 rpm for 1.5 h. The resulting NRL/MWCNTs mixture (30 mL) was filtered under vacuum through a cellulose ester membrane to form a thin film. After washing with deionized water and soaking in acetone to dissolve the cellulose ester membrane, the film was dried at 60 °C for 1 h. The resulting NRL/MWCNTs film was cut into 10 mm×15 mm rectangles, stacked face-to-face，and the D-MN was obtained. The subsequent fabrication steps for the sensor are the same as P-MN_3@D-MN sensor.

Characterizations

Fourier transform infrared spectroscopy (FT-IR) was carried out on a Bruker Tensor 27 spectrometer (Bruker Optics, Germany) using attenuated total reflectance (ATR) mode from 4000 to 600 cm^{-1} with a resolution of 4 cm^{-1} and scanning times of 32. Element composition analysis was carried out on an energy dispersion spectroscopy (EDS, X-MaxN 20, Oxford Instruments, Britain) accompanied by SEM. Raman spectra was conducted by inVia Reflex (532 nm, Renishaw, Britain) in the range of 100-3200 cm^{-1}. The surface morphologies of the sponges were examined using a field emission scanning electron microscope (SEM, Merlin, Carl Zeiss Jena, Germany) with an acceleration voltage of 15.0 V. The sample preparation method for cross-sectional SEM

characterization involved rapidly freezing the test samples in liquid nitrogen and then fracturing them. Water contact angles (WCAs) were measured by a contact angle meter (DSA25, Kruss, Germany) using a 4 μL water droplet as probe liquid at room temperature. Each WCA was tested for at least three different locations to calculate the average value.

Sensing performances of the sensor and its application in human motion and detection in underwater/simulated seawater environments

The sensing performances of the piezoresistive pressure sensors were studied using a two-point probe multimeter (DMM6500, Keithley, USA) connected with a universal testing machine (ESM303, Mark-10, USA). The relationship between pressure strain or bending angle and relative resistance change (RRC, %) of the sensor changed as the pressure increased. The piezoresistive pressure sensor was respectively attached on the fingers, ankle joints, face and throat of a 25-year-old healthy male tester with a weight of 75 kg and a height of 181 cm by tape, and the electrical resistance change of the sensor caused by various motions and pronunciation were recorded by the multimeter.

To simulate the sensing environment under water and seawater, the sensor was placed 5 cm below the surface of liquid in a beaker. The liquid were tap water (conductivity 600 $\mu S\ cm^{-1}$) and simulated seawater (NaCl concentration 36 $g\ L^{-1}$, conductivity 65 $mS\ cm^{-1}$), respectively.

In the seawater sensing stability test, the sensor was placed at the bottom of a tank with a height of 40 cm full of simulated seawater (NaCl concentration 36 $g\ L^{-1}$, conductivity

65 mS cm^{-1}). Three heating magnetic stirrers were placed under the tank and three magnets (520 rpm) were used in the tank to generate water flow fluctuations at the bottom. The resistance change of the sensor was continuously monitored by a resistance-capacitance signal acquisition system (01RC, Linkzill, China). The sensing data was transmitted to a cellphone via a built-in Bluetooth feature.

Tab. S1 Key metrics of P-MN_3@D-MGN sensor and other natural-polymer-based pressure sensors

Natural-polymer-based pressure sensors	Stability (cycle number, n)	Response time (ms)	Recovery time (ms)	Sensitivity (kPa^{-1})
Bacterial Cellulose/MXene[1]	5000	170	266	125.8 (based on $\Delta I/I_0$)
Bacterial Cellulose/Chitosan/GO[2]	3000	120	90	150.0 (based on $\Delta I/I_0$)
Alkalilignin/PVA/MTMS/ PEDOT[3]	10000	46	37	0.7 (based on $\Delta R/R_0$)
Cellulose nanofiber/MWCNT[4]	1000	200	300	6.1 (based on $\Delta I/I_0$)
Loofah fiber fabric/MWCNT[5]	5500	64	68	30.8 (based on $\Delta I/I_0$)
Silk fibroin/aramid nanofibers/Au[6]	1200	--	--	23.8 (based on $\Delta R/R_0$)
Cotton fiber/MXene[7]	5000	80	40	17.7 (based on $\Delta R/R_0$)
This work (NR/MWCNTs)	20000	20	53	96.0 (based

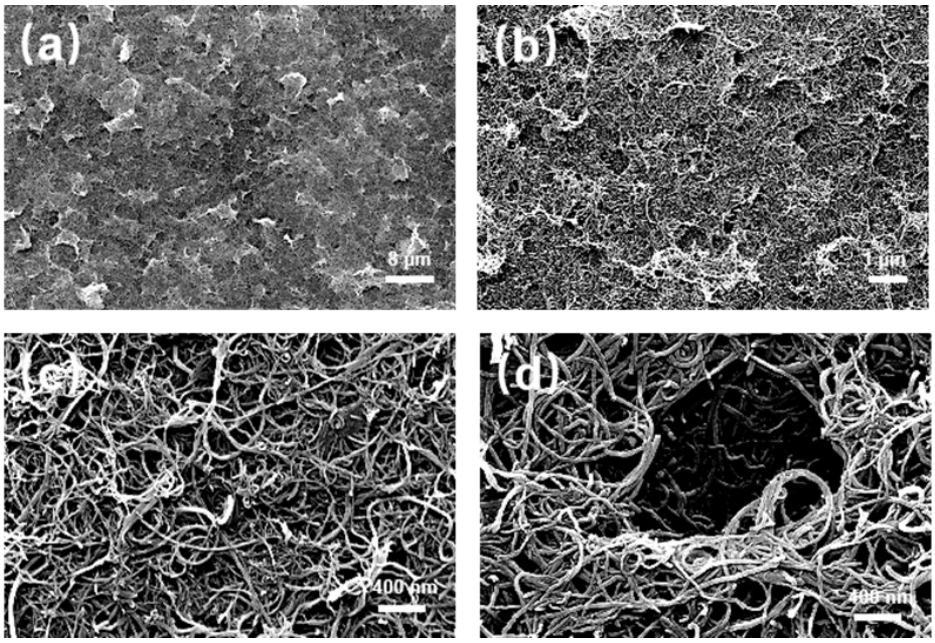

Fig. S1 SEM images of the GEL/MWCNTs film surface at (a) 2000×, (b) 10000×, (c) 30000× and (d) 50000× magnifications.

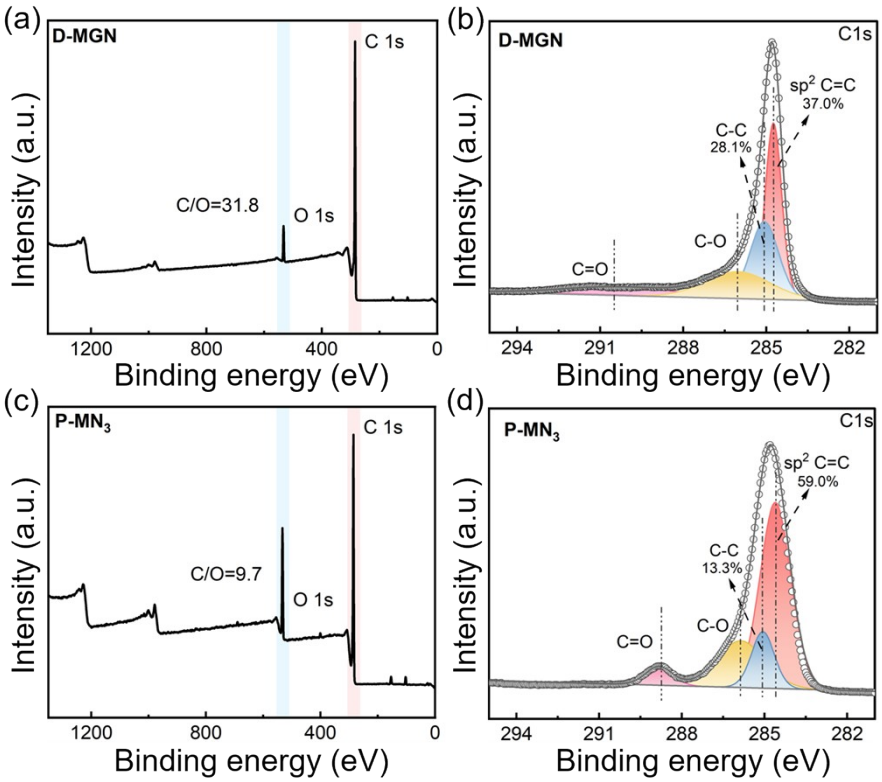

Fig. S2 (a) XPS spectrum and (b) C 1s spectrum of D-MGN sensitive interlayer. (c) XPS spectrum and (b) C 1s spectrum of P-MN_3 protective layer.

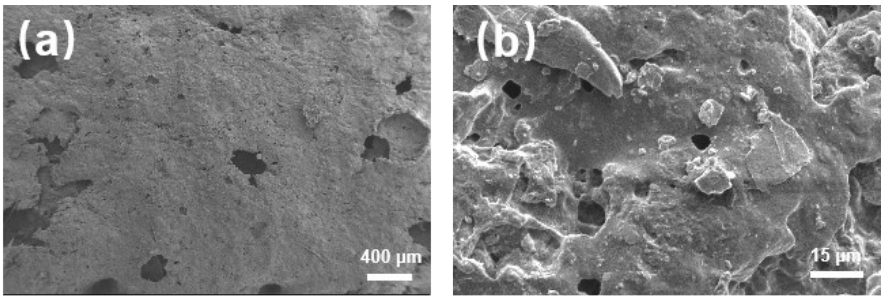

Fig. S3 SEM images of the NR/$NaCl_{1:1}$ protect layer surface at (a) 30×, (b) 10000× magnifications.

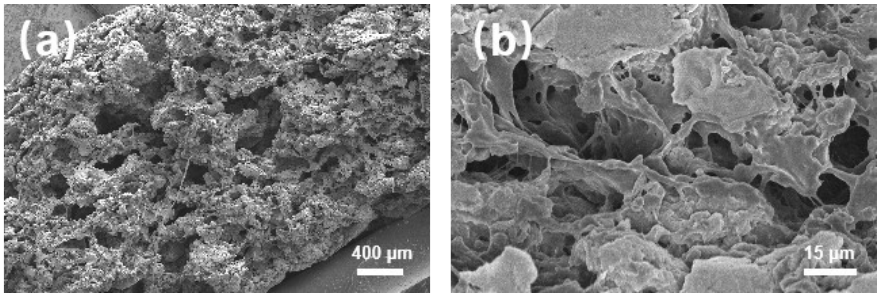

Fig. S4 SEM images of the NR/$NaCl_{1:6}$ protect layer surface at (c) 30× and (d) 600× magnifications.

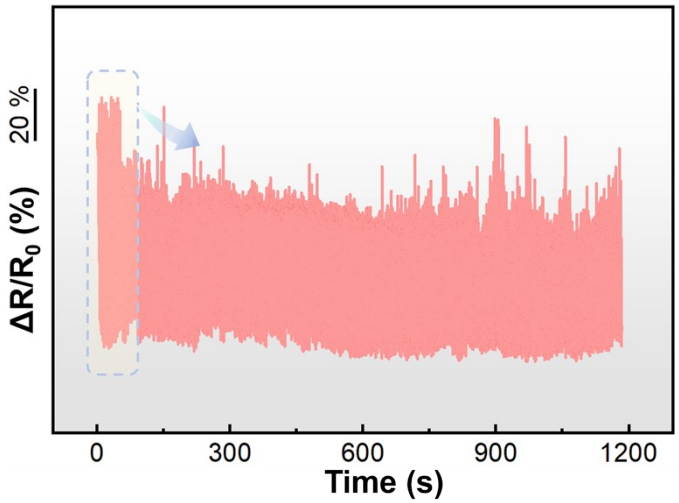

Fig. S5 RRC curve of P-MN_3@D-MN sensor during loading-unloading cycles under 0-4.5 kPa.

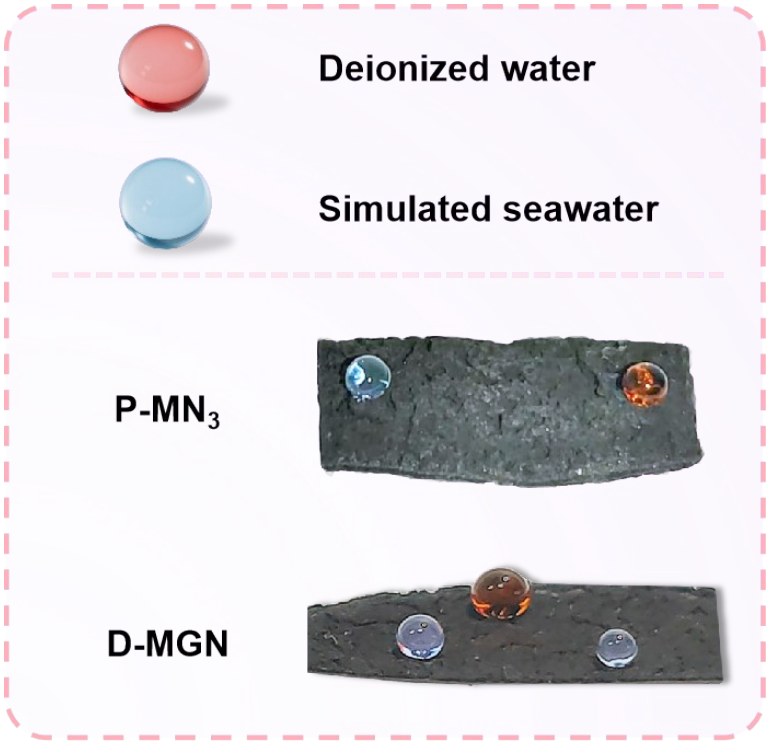

Fig. S6 Deionized water and simulated seawater droplets on P-MN_3 porous protective layer and D-MGN sensitive interlayer.

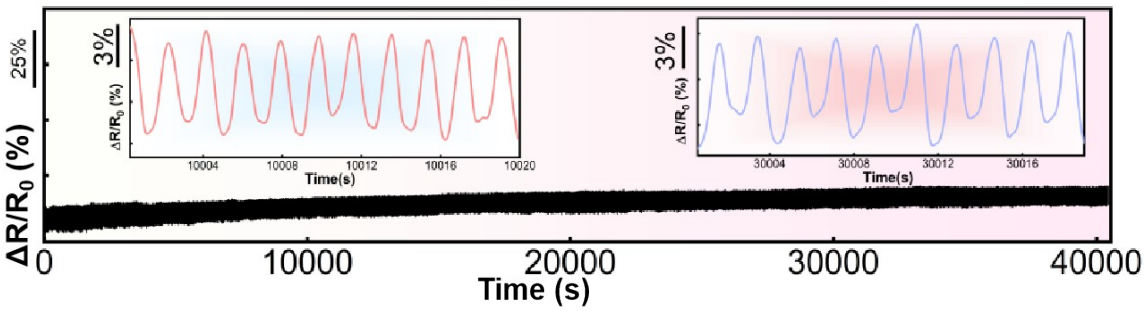

Fig. S7 Relative resistance change during 15000 bending cycles at 0-13°.

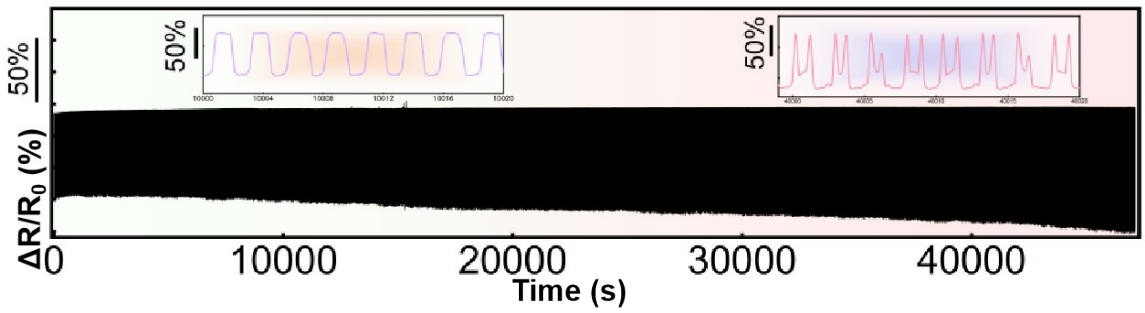

Fig. S8 Relative resistance change during 10000 stretching-releasing cycles at 0-1% strain.

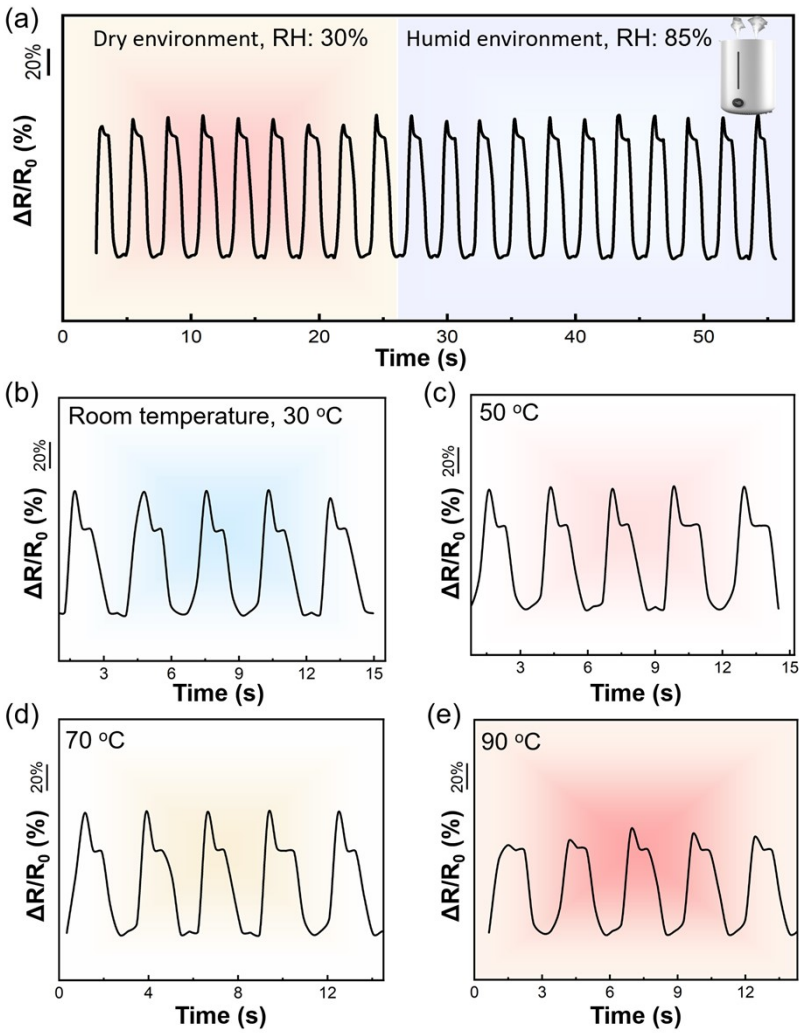

Fig. S9 RRC curves of the sensor under (a) different relative humidity of 30% and 85% and different temperatures of (b) 30 °C, (c) 50 °C, (d) 70 °C, and (e) 90 °C, respectively.

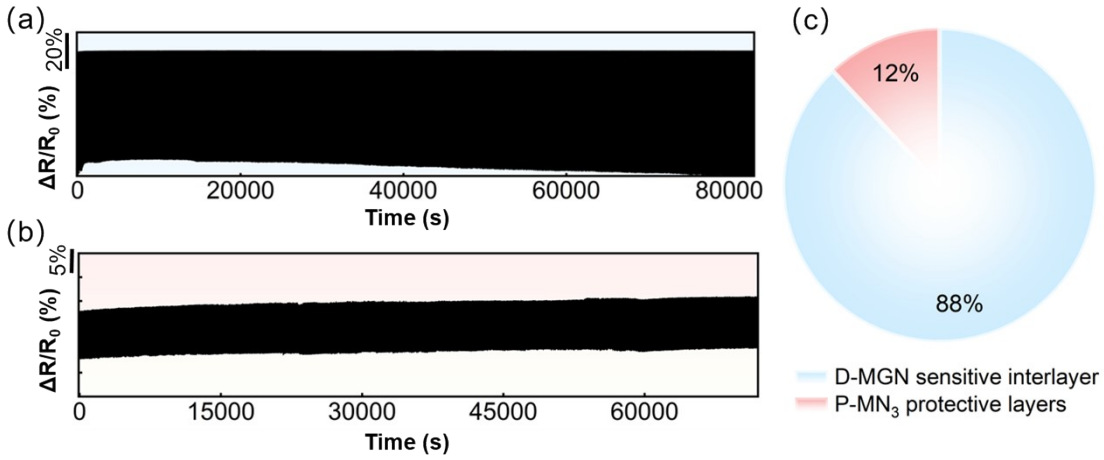

Fig. S10 RRC curve of (a) D-MGN sensor and (b) P-MN_3 sensor during loading-unloading cycles. (c) Contributions from protective layers and sensitive interlayer to the resistance change of the sensor.

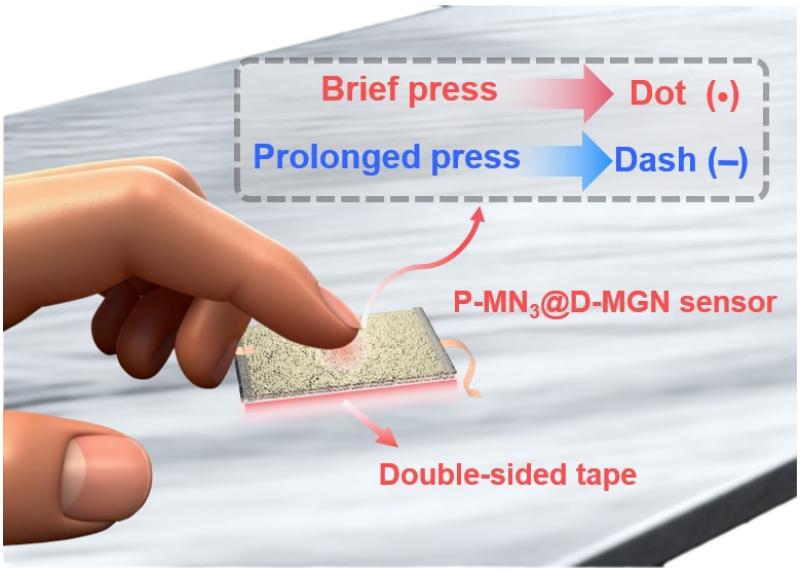

Fig. S11 Schematic of Morse-code transmission application of P-MN_3@D-MGN sensor.

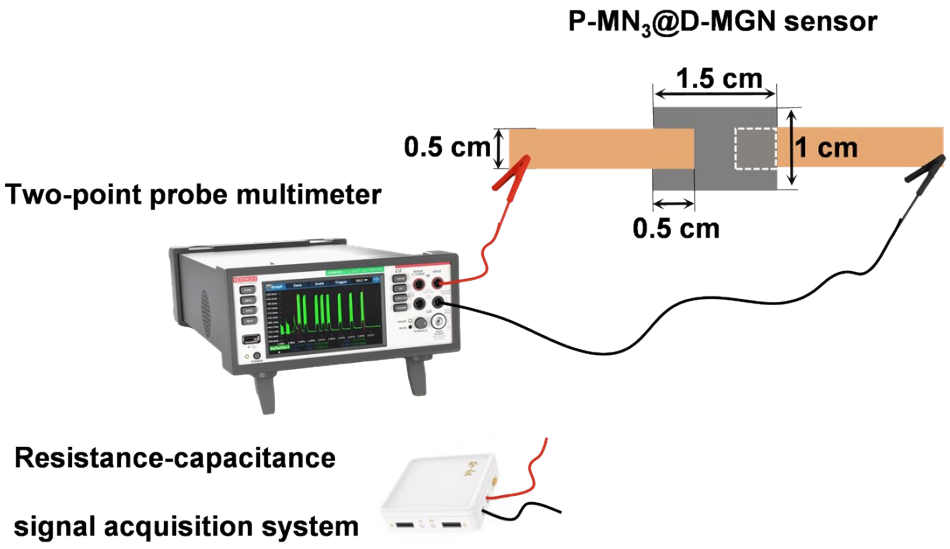

Fig. S12 P-MN_3@D-MGN sensor, electrodes and integration schematic.

References

1 X. Jin, L. Li, S. Zhao, X. Li, K. Jiang, L. Wang and G. Shen, *ACS Nano*, 2021, **15**, 18385-18393.

2 Q. Xiang, H. Zhang, Z. Liu, Y. Zhao and H. Tan, *Chem. Eng. J.*, 2024, **480**, 147825.

3 W. Han, S. Wang, M. Zhang, K. Long, W. Zhang, C. Dai, J. Wang and J. Huang, *J. Mater. Sci. Technol.*, 2026, **253**, 39-50.

4 X. Du, Q. Chen, Q. Zhou, Y. Zhou, F. Wang, W. Xu, Y. Zhan and M. Jiang, *Compos. Sci. Technol.*, 2025, **260**, 110976.

5 C. Lu, Y. Shen, X. Chan, S. Yu, L. Hu and L. Li, *Small*, 2025, n/a, e06521.

6 S. Linghu, S. Chen, J. Cheng, T. Wang, Y. Bu, P. Wang and L. Chen, *Compos. Sci. Technol.*, 2025, **268**, 111206.

7 H. Pan, G. Chen, Y. Chen, A. Di Carlo, M. A. Mayer, S. Shen, C. Chen, W. Li, S. Subramaniam, H. Huang, H. Tai, Y. Jiang, G. Xie, Y. Su and J. Chen, *Bios. Bioelectron.*, 2023, **222**, 114999.